eng

MDPI

Article

Ultrasonic Effects on Foam Formation of Fruit Juices during Bottling

Julian Thünnesen [1,*], Bernhard Gatternig [1,2,3] and Antonio Delgado [1,2]

[1] Institute of Fluid Mechanics, Friedrich-Alexander University Erlangen-Nuremberg, Cauerstr. 4, 91058 Erlangen, Germany; bernhard.gatternig@fau.de (B.G.); antonio.delgado@fau.de (A.D.)
[2] German Engineering Research and Development Center LSTME Busan, Busan 46742, Korea
[3] Hochschule Weihenstephan·Triesdorf, Verfahrenstechnik und Kreislaufwirtschaft, Markgrafenstr. 16, 91746 Weidenbach, Germany
* Correspondence: julian.thuennesen@fau.de

Abstract: Non-carbonated fruit juices often tend to foam over during bottling. The resulting foam height corresponds to the equilibrium of foam formation and decay. Therefore, the foam unexpectedly occupies more space in the bottle and carries parts of the juice out of the bottle, resulting in product loss under filled containers and hygienic problems in the plant. Chemical antifoams are likewise undesirable in most cases. Recent ultrasonic defoamers are effective but only capable outside the container and after the filling. In this article, a lateral ultrasonication through the bottle wall with frequencies between 42 and 168 kHz is used in-line for non-invasive foam prevention during filling. Foam formation during hot bottling of orange juice, apple juice, and currant nectar at 70 °C happens at flow rates between 124–148 mL/s. The comparably high frequencies have a particular influence on the fresh foams, where a large fraction of small resonant bubbles is still present. Foam volume reductions of up to 50% are reached in these experiments. A low power of 15 W was sufficient for changing the rise of entrained bubbles and minimizing the foam development from the start. The half-life of the remaining foam could be reduced by up to 45% from the reference case. The main observed effects were a changed rise of entrained bubbles and an increased drainage.

Keywords: ultrasound application; glass bottles; fruit juice; foam drainage; foaming behavior

check for updates

Citation: Thünnesen, J.; Gatternig, B.; Delgado, A. Ultrasonic Effects on Foam Formation of Fruit Juices during Bottling. *Eng* **2021**, 2, 356–371. https://doi.org/10.3390/eng2030023

Academic Editor: Angeles Blanco Suarez

Received: 5 July 2021
Accepted: 9 September 2021
Published: 14 September 2021

1. Introduction

In the food and beverage industry, products tend to foam up unintentionally during processing due to their chemical composition. This phenomenon can be observed in the bottling not only of carbonated beverages but also of non-carbonated fruit juices. Similar to everyday pouring into a jar, in the worst case, the foam increases in volume disproportionately to the actual liquid poured in, takes up the planned space in the vessel, and threatens to overflow. Particularly in the process of hot filling already-pasteurized beverages into glass bottles, the containers are sometimes considerably underfilled, as the headspace fills with foam before the required legal minimum volume has been reached. Below this volume, a bottle of this type may not be sold, which means that the economic loss corresponds with a loss in sales price. The result is lower line efficiency by up to 5%, underfilling of the containers, higher production losses, and greater cleaning efforts for the line. Therefore, it is already of interest to medium-sized companies to increase plant utilization by even 1% through foam prevention and thus save up to €50,000 per year [1].

In practice, it is only possible to passively reduce foam formation by reducing the filling speed, since a decreased velocity of the free jet carries less gas from the headspace into the liquid. The entrained bubbles rise to the surface and agglomerate to form the foam. The resulting foam height is obtained from the net foam balance, which is the time ratio of foam formation to foam decay. Especially in the short time window of a few seconds for bottle filling, foam decay is dominated by drainage, where films and plateau edges lose liquid and decay below a critical thickness [2–4]. Deposited particles, e.g., from pulp, and capillary forces in the plateau areas inhibit drainage; hence, foam persists longer than the time window permits. Naturally fluctuating material properties of the juices, such as the content of proteins, polyphenols, sugars, and soluble solids, etc., constantly change the formation and half-life of the foam, which is why it is constantly necessary to manually adjust the filling speed to avoid over-foaming despite optimized filling tube geometries [5–10].

A method of active and adaptive foam destruction during filling is currently not found in literature or in practice. A look at other industrial fields reveals chemical, thermal, and mechanical defoaming methods, but most of these are not applicable to bottling. Chemical methods, such as the use of defoamers, are limited due to strict national food laws and face the disadvantage of more expensive and environmentally hazardous consequences [11,12]. Therefore, mechanical foam destruction based on ultrasonic waves is of particular interest.

Ultrasound is noninvasive and propagates as a mechanical wave in gases, liquids, and solids, creating localized pressure differences. It is assumed that ultrasonic waves penetrate the lamellae, atomize the liquid from the lamellae, or hit the resonant frequencies of the bubbles, creating surface waves along the lamellae and enhancing drainage [13–17]. Current knowledge on ultrasound-based foam destruction is largely based on laboratory experiments with airborne ultrasound. Ultrasonic foam destruction was initially studied using sirens and Hartman whistles [18–20]. The frequency range from audible 0.7 to 29 kHz showed effective defoaming only at sound power levels of at least 145–148 dB [21]. Additional work on foam control in fermentation vessels showed that defoaming ability increased with higher frequencies from 26 to 34 kHz and rapidly disintegrated foam at high sound intensities of 10 W/cm^2 or 120 dB [20]. More recent work has investigated airborne sonication of the foams with piezo-acoustic actuators [14–16,22]. Most of the works used a sonotrode with a frequency of 20 kHz and considered the degree of defoaming dependent on the foam and power applied. It was found that ultrasound is more effective with decreasing viscosity and is just suitable for aqueous foams with average bubble diameters of 0.5–5 mm. However, higher foam formation rates and water contents in the case of foams with SDS required stronger amplitudes, since the liquid migrates only to the neighboring plateau areas when the top foam layer is destroyed and the foam thus loses little liquid hold-up [22,23]. With increasing liquid hold-up and lamella thickness, the reflection coefficient at the foam interface increase. The acoustic power to be applied is so high that Dedhia et al. [22] considered pulsed sonication in terms of economy.

However, for an inline application during filling, airborne high-power ultrasound has several significant drawbacks. For very wet foams, defoaming should not occur by cavitation formation and atomization of the liquid in the lamella. On the one hand, the generation of transient cavitation for a decent foam decay requires a sound intensity of about 100 W/cm^2, which is equivalent to a burnout of an heating wire for boiling water. This negatively influences the energy efficiency of the plant, and thermal product degradation could occur. On the other hand, the product is partially atomized, and an aerosol is produced that contaminates the filling system and thereby causes hygienic problems [24]. At the same time, these methods require ultrasonic actuators with relatively large diameters compared to common bottle dimensions. As a result, due to the limited accessibility to the foam and the small installation space, the sonotrode can only remove the excess foam after filling [14,15].

Apart from airborne insonication, Winterburn and Martin [25] demonstrated that sonication via the liquid also accelerates drainage at 40 kHz and at already 4 W total electrical power, as the impedance between air and water is improved. Although the pressure amplitude was too low to rupture the lamellae in the experiments, as is assumed for airborne ultrasound [14], the authors detected stronger effects at 40 kHz than at 28 kHz. However, a fundamental understanding of the mechanisms of foam destruction is lacking.

This leads to the research question of an innovative, energy-efficient, and product-friendly alternative in the form of a resonance-based method of foam destruction for beverage filling using ultrasound. By using resonant effects, the acoustic power and thus the energy consumption can be significantly reduced. High temperatures and peak pressures from cavitation events no longer occur; thus, product degradation and aerosol formation may not occur. The lower power requirements allow for a coupling of the ultrasound transducer through the bottle wall and liquid phase, giving plant designers more flexibility for system integration.

The primary resonance excitation in foam promotes the generation of surface waves and lowers the viscosity of the liquid in the lamellae. Drainage increases, causing the dynamic foam height to be lower. In published literature, ultrasound has been used in food foams only to determine bubble size distribution and gas content, thus providing information on the frequency-specific resonance behaviors of bubbles [26–28]. In all work, bubbles are assumed to absorb sound in a frequency-specific manner and oscillate in the process. However, it is not yet fully understood how the resonance effects behave within the foam regarding to enhance defoaming. On the one hand, an increasing gas content in the foam lowers the resonant frequency of a bubble [28], while the presence of neighboring resonant bubbles at a distance of half a wavelength would increase the frequency [29]. In the latter case, bubbles with a radius of about 100 µm would resonate at 86 kHz instead of 31 kHz with a gas content of 26%.

The article addresses the following research objectives: (i) discovering which ultrasonic frequencies can minimize the resulting foam height during filling due to resonance effects. Frequencies that are still high enough to keep the potential of transient cavitation low (>40 kHz) and low enough that their wavelengths roughly correspond to the theoretical resonance lengths of the smallest lamellae or bubbles (<200 kHz) are considered. The bubble fractions, which tend to be smaller, are usually located at the bottom of the foam, which is why objective (ii) is whether sonication of the liquid through the wall of the bottle from the side or bottom can achieve the desired effect. This promises no aerosol formation and a lower transmission loss than with the air gap between the transducer and the foam. Finally, for objective (iii), the required ultrasound power and duration of sonication are investigated to deduce the energy requirements of the process. The results are considered in terms of industrial feasibility.

2. Materials and Methods

2.1. Experimental Set-Up

The aim of the tests was to investigate the influence of different frequencies on foam formation during atmospheric filling under realistic conditions. The test conditions were based on the standard filling specifications for fruit juices in refillable glass bottles, in which a maximum filling time of 10 s is specified. The required volume flow was achieved via the height difference between the reservoir tank (100 × 100 × 250 mm) and the filling tube opening of 930 mm (Figure 1).

Before each filling, 1.2 L of the juice, previously tempered to 70 °C, was taken from a thermobath (3 L) to a reservoir tank. This quantity of juice allowed for the avoidance of additional air intake into the pipe towards the end of the filling.

A magnetic valve and a flow meter below the reservoir tank controlled the filling interval and recorded the flow rate, respectively. The juice entered the bottle via a height-adjustable filling nozzle (length: 250 mm, inner diameter 8 mm). The adjusted height between the nozzle outlet and the bottom of the bottle was 250 mm for the trials with apple juice and currant nectar. For orange juice, the filling nozzle was set at a height of 50 mm. This allowed the foam heights within replicates to be kept as low as possible.

A CCD camera (acA2500-60 uc, Basler GmbH, Ahrensburg, Germany) recorded foam formation at 1 fps during filling. Control of the valve and data recording were done centrally via a mini-PC (Raspberry Pi 4 Model B). The sampling period of all sensors was synchronized to the camera's recording rate and was 1.03 s between samples.

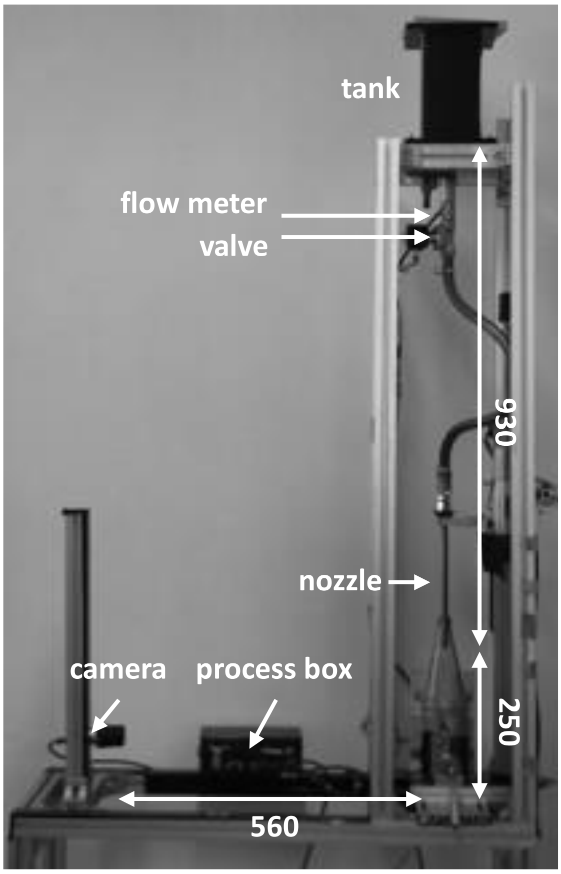

Figure 1. Filling setup (here: without heating bath) with given distances [mm].

The individual filling cycles were divided into fixed time periods: initialization (1 s), filling (10 s), and decay (9 s) phases. During the filling phase, the volume flows were kept constant for each of the juices (Table 1). After the filling phase, the decay phase additionally served to assess the pure foam decay during sonication.

Table 1. Measured flowrate of currant nectar, apple juice, and orange juice at 70 °C.

Flowrate (L/s)	Black Currant	Apple	Orange
Mean (n = 630)	0.1277	0.1361	0.1480
Std (n = 630)	0.0015	0.0059	0.0045

The vessel used was a 300 mm high commercial glass bottle (model: 1 L VdF bottle) consisting of a 149 mm high cylinder and a cone above it. After measuring three different bottles with a caliper, the inner radius r can be described as a function of the height h:

$$r(h)[\mathrm{mm}] = \begin{cases} 43.75, & h < 149 \text{ mm} \\ 0.207 * (149.5 - h) + 43.75, & h \geq 149 \text{ mm} \end{cases} \quad (1)$$

A clamp fixed the bottle to the ultrasonic actuator on the side, which rested against the cylindrical wall of the bottle at a height of 30–70 mm (Figure 2a).

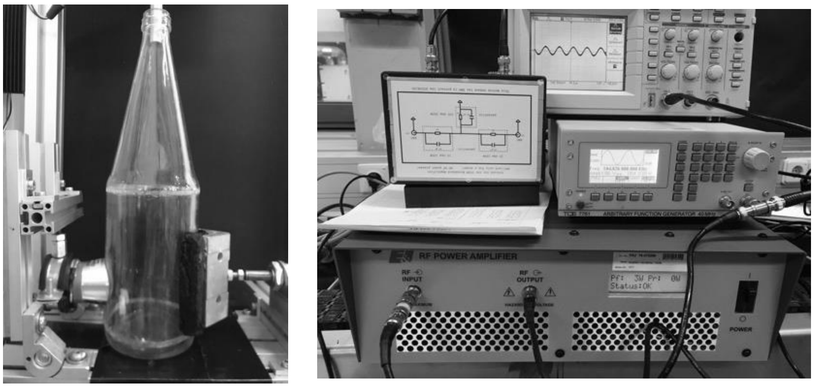

(**a**) (**b**)

Figure 2. Fixing device for the bottle to the modified transducer (**a**) and amplifier system (**b**).

The ultrasonic transducer was a modified 40 kHz Langevin transducer (Hesentec, Rank E), which had a front face adapted to the curvature of the bottle wall (radius r = 44 mm). This modification changed the resonant frequencies of the transducer to 42, 56, 85, 101, and 168 kHz. A arbitrary function generator (TOE7761, Toellner, Herdecke, Germany) produced a sinusoidal signal of the corresponding frequency, which was amplified by 51 dBV through a voltage amplifier (1040 L, Electronics and Innovation, LTD, Rochester, NY, USA). A parasitic resistor box was connected between the amplifier and the transducer to protect the amplifier from changing impedances of the transducer (Figure 2b).

Power outputs at 10, 15, and 20 W_{el} were investigated. The maximum generated pressure amplitudes inside a filled bottle are shown in Table 2 according to hydrophone measurements.

Table 2. Maximum pressure amplitudes of output frequencies.

W_{el}	p ($\times 10^5$ Pa)				
	42 kHz	**56 kHz**	**85 kHz**	**101 kHz**	**168 kHz**
10	1.033	0.078	2.376	0.761	0.666
15	2.284	0.1	3.036	1.332	0.772
20	2.773	0.119	3.63	1.543	0.772

2.2. Juices

Orange juice (100% fruit content with pulp, Erwin Dietz GmbH, Osterburken, Germany), filtered apple juice (100% fruit content, Erwin Dietz GmbH, Osterburken, Germany), and currant nectar (25% fruit content, Granini, Nieder-Olm, Germany) tempered to 70 °C were used.

Their density, viscosity, and surface tension were triply determined using a hydrometer, a capillary viscometer, and a contact angle meter (Wilhelmy plate method, K100, Krüss, Hamburg, Germany) at 70 °C as shown in Table 3.

Table 3. Density, viscosity, and surface tension of apple juice, orange juice, and currant nectar at 70 °C.

	Density (kg/m^3)	**Viscosity (mPa $\times$ s)**	**Surface Tension (mN/m)**
Apple juice	1014.82	0.498	28.06
Orange juice	1011.50	2.344	26.85
Black currant nectar	1018.50	0.450	38.47

2.3. Statistical Methods

A total of 108 fillings were considered with six replicates per juice, power level and frequency. Results are given as means with standard deviations. For the statistical evaluation with a two-factorial ANOVA and the calculation of the Spearman correlation coefficient in Excel 2016, the foam heights at time t = 8 s were used. At this time, the foam is still in the cylindrical region of the bottles and is not yet affected by the increasing influences during bottle tapering, which would shift the normal distribution to a right-handed one. A two-factor ANOVA (Excel 2016) revealed that trials differed between juices (p-value = 2.51×10^{-42}), sonication significantly decreased foam (p-value = 1.86×10^{-11}), and interactions between frequencies and juices also occurred (p-value = 1.035×10^{-16}).

2.4. Measurement of Foam Heights

The temporal development of foam was recorded via the camera's image series. Only the pixel lengths in vertical direction were considered. To this end, constant heights of the bottle opening $y_{bottle,\ top}$ and bottom $y_{bottle,\ bottom}$ were measured once for each run, and the heights of the top and bottom edges of the foam were determined ($y_{foam,\ top}$ and $y_{foam,\ bottom}$) for the individual images. The origin of the coordinate system in the image is in the upper left corner, thus accounting for the y-values increase towards the bottom. The process was performed using a semi-automated script in OpenCV, i.e., foam edges were manually selected and the according y-values were calculated and saved automatically. The resulting foam height h_f and liquid height h_l were calculated by taking the difference of the respective y-values and including the conversion ratio R of the image.

$$R\left[\frac{Px}{mm}\right] = \frac{y_{bottle,\ bottom} - y_{bottle,\ top}}{h_{bottle}} \tag{2}$$

$$h_l\ [mm] = \frac{y_{bottle,\ bottom} - y_{foam,\ bottom}}{R} \tag{3}$$

$$h_f\ [mm] = \frac{y_{foam,\ bottom} - y_{foam,\ top}}{R} \tag{4}$$

Finally, the foam volume was calculated from the volume of a truncated cone with the radii according to equation 1 and the foam height. In the region between the cylinder and cone at h_l < 149 mm and $h_l + h_f$ > 149 mm, the foam volume was the sum of a truncated cone of a height $h_1 = (h_l + h_f - 149\ \text{mm})$ and a cylinder of $h_2 = (149\ \text{mm} - h_f)$.

2.5. Uncertainty Analysis of Measurements

The heights of the bottle, foam, and liquid were dependent on the accuracy of the computer display. At the same time, the edges of the foam in the image were not always horizontal, resulting in measurement uncertainty when measuring the average height.

The single-sample analysis by Moffat calculated the uncertainties separately. Measurements of two filling tests with 20 images each provided the data. Each bottle edge was measured in the respective image. For the changing foam and filling heights, the y-values were determined tenfold in each image. The uncertainties were caused by the repetition and measurement errors by the author and are indicated by the standard deviation σ:

$$\sigma = \sqrt{\frac{1}{(N-1)} \sum_{j\,=\,1}^{N} \left(\overline{y} - y_j\right)^2} \tag{5}$$

The standard deviations are shown in Table 4. The relative errors of the foam edges varied depending on the fill level, which is why they are not shown in the table. Instead, the relative errors of the foam height based on them are given later.

Table 4. Uncertainties dX_i and the relative uncertainties $\frac{\sigma}{X_i}$ of individual measured variables X_i, given in the respective units, n = 40.

δX_i	$\delta X_i{=}\sigma$	$\frac{\sigma}{X_i} \times 10^2$ [%]
$y_{bottle,\ bottom}$ [Px]	3.16	0.21
$y_{bottle,\ top}$ [Px]	1.71	2.12
$y_{foam,\ bottom}$ [Px]	2.76	
$y_{foam,\ top}$ [Px]	5.45	
bottle height [mm]	0.50	0.2

The uncertainties contributed by multiple input variables were calculated by a combination of the root-sum-square method:

$$\delta R = \sqrt{\sum_{i\,=\,1} \left(\frac{\delta R}{\delta X_i} \sigma \right)^2} \tag{6}$$

where the measurement uncertainty δR, is characterized by the individual uncertainties of the measured variables $\delta X_i = \sigma$. To calculate the uncertainties of the conversion ratio, the foam and the liquid height, the Equation (2) were, respectively, put into (3) and (4) and partially derived according to the individual variables X_i.

For the conversion coefficient R, the measurement uncertainty was δR = 0.014 Px/mm and a relative error of 0.31%. Table 5 shows the absolute measurement uncertainties of the liquid height δh_l and the foam height δh_f, as well as their relative deviations for representative heights, respectively.

Table 5. Uncertainties dX_i and the relative uncertainties $\frac{\sigma}{X_i}$ at given values of liquid height h_l and foam height h_f.

Liquid Height h_l			Foam Height h_f		
X_i (mm)	dX_i (mm)	% error	X_i (mm)	dX_i (mm)	$\frac{\sigma}{X_i} \times 10^2$ (%)
99.93	1.39	1.24	5.40	1.36	25.20
88.87	1.38	1.37	9.93	1.36	13.70
77.82	1.38	1.54	18.13	1.36	7.50
66.77	1.37	1.75			
55.72	1.37	2.03			
44.67	1.37	2.43			
33.62	1.36	3.03			
22.57	1.36	4.02			
11.51	1.36	5.98			
0.46	1.36	11.71			

Deviations < ±1.37 mm around the mean foam heights shown below are due to measurement uncertainty. Above the value, the deviations are attributable to the system.

3. Results and Discussion

3.1. Evolution of Foam Formation

During the filling phase, three phases of foam formation were evident in all reference tests of the juices (see Figure 3). Initially, the filling jet hit the bottom of the bottle, causing the juice to rise radially along the bottle wall and trap air as it falls back to the center. The flow is chaotic in the first second, which means that the liquid level is not horizontal. Almost two seconds later at a filling height of 45 mm, the entrapped bubbles rise to the surface and form the first layer of foam. In the following phase, continuous foam formation occurs in the cylindrical part of the bottle due to the introduced of air by the free jet. The foam formation happens almost constantly during this phase. The free jet deforms the gas–liquid interface and causes the formation of gas pockets. If the destabilizing inertial forces caused by the free jet outweigh the stabilizing surface forces, the interface is strongly deformed and bubble entrapment occurs [17]. According to the literature, the gas entrapment shows a nonlinear dependence on the liquid volume flow rate [17]. At the same time, foam development depends on the ascent time of the bubbles rising to the surface. This time either depends on the diameter of the gas bubbles, the viscosity and density of the juice, or the ratio of bubble ascent speed to filling speed. In the case of orange juice, no additional gas entrainment occurred at a filling level of 50 mm due to the already immersed filling nozzle. As such, the foam volume remained constant with some delay due to rise of the bubbles from the 70 mm filling level.

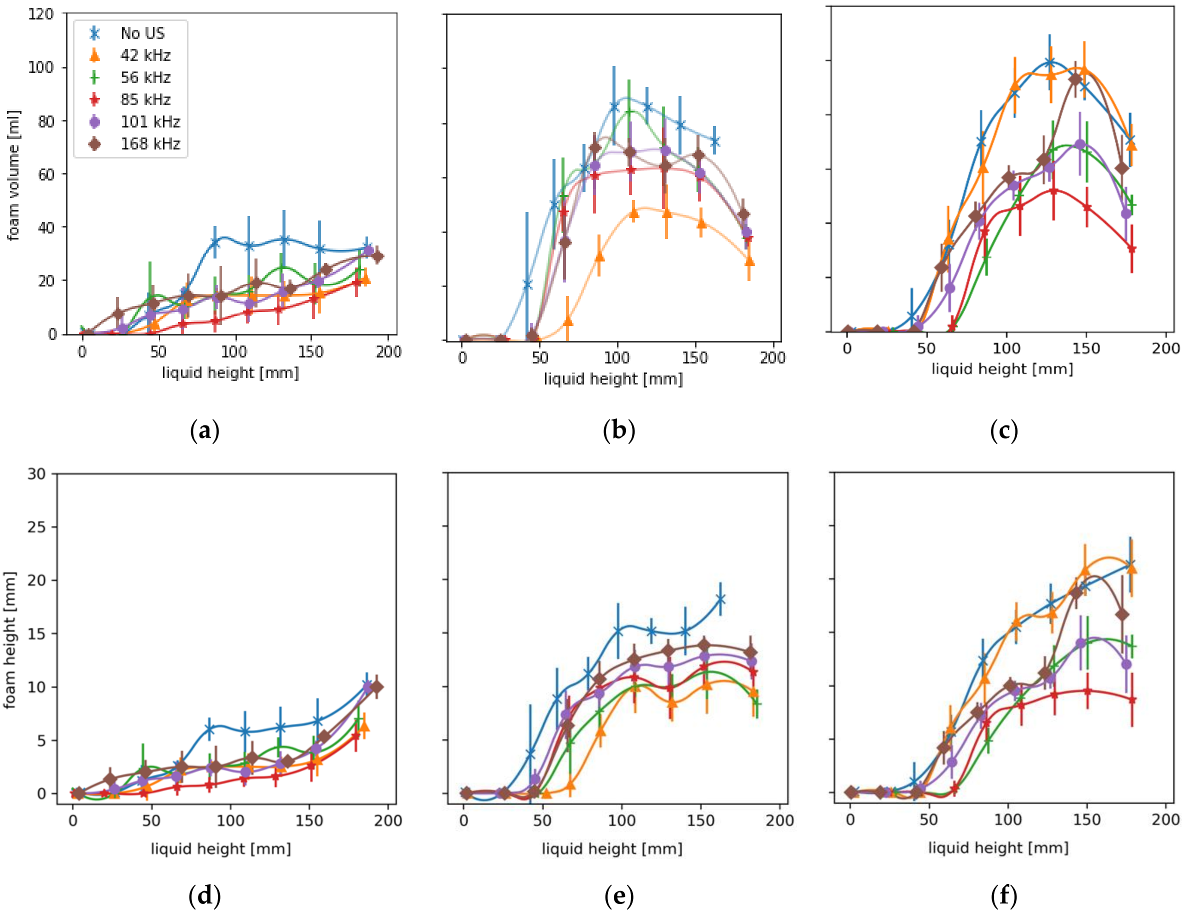

Figure 3. Effect of frequency dependent, permanent ultrasound insonication on the evolution of foam volume (**a**–**c**) and foam height (**d**–**f**) for orange juice (**a**,**d**), apple juice (**b**,**e**), and currant nectar (**c**,**f**), each at 70 °C, n = 6.

In the final phase, the foam enters the cone at a height of 149 mm where the foam volume remains constant in the case of orange juice and decreases in the case of apple juice and currant nectar. Due to the cross-sectional taper of the cone, shear forces along the wall crushed larger bubbles in the foam. This shear causes a reduction in volume but not to the extent that it causes the foam heights to remain constant while the cross-sectional taper is reduced (compare Figure 3).

The effectiveness of forced foam decay was very consistent at power levels 10, 15, and 20 W, while it showed a larger dependency on frequency. Therefore, the presented results of 15 W also represents the other power levels. As seen in Figure 3, sonication immediately causes less foaming at a liquid level between 45 and 70 mm. The delayed and lower foaming that occurred initially was independent of the frequency, height of the filling nozzle, and juice, but this differs somewhat in the later phases. With a low nozzle attachment for orange juice, the frequencies 42, 56, and 85 kHz are most effective.

Specifically, sonication at 42 and 85 kHz delays formation until filling is concluded and causes a lower foam height. The higher frequencies, 101 and 168 kHz, only allow more foam formation from a filling height of 130 mm compared with the reference tests.

In the case of a high nozzle attachment for apple juice and currant nectar, sonication also caused a delayed foam formation. Especially in apple juice, the frequencies 42, 85, 101, and 168 kHz significantly reduced foam formation at 80 mm filling level when the transducer fully submersed in the liquid. Furthermore, ultrasound at frequencies 56, 101, and 168 kHz reduced foam formation also in currant nectar. The frequency of 85 kHz is particularly effective here, where the first foam just formed at 70 mm. Meanwhile, 42 kHz provoked a higher foam volume.

As aforementioned, foam formation primarily happened through gas entrainment of the free jet, whose generated bubble size distribution depends on the viscosity, density, and surface tension of the respective juice. Accordingly, the foam characteristics are dependent on the respective juices. Figure 4 shows the resulting foam heights after filling against the applied sonic frequency and density of the respective juice. The main influence of the foam's height happened along the density. This is obvious in the case of orange juice and a lower filling nozzle. However, it is interesting to note that, compared with the respective reference tests, sonication reduces the foam height by about 50% on average at frequencies between 42 and 101 kHz. This reduction becomes less at 169 kHz.

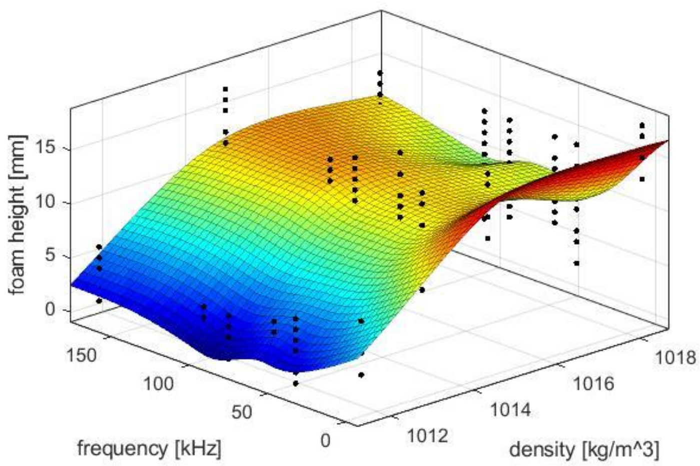

Figure 4. Resulting foam heights after filling at t = 8 s plotted against the density of the juice and the frequency used.

Figure 4 accordingly shows that the absolute foam height at the end of the respective filling at t = 8 s differs between the respective juices but is consistently reduced by the respective frequencies. Especially the frequencies 85 and 101 kHz reduce foam within a respective juice.

Figure 5 shows that the foam formation of apple juice and currant nectar is less inhibited by a delayed sonication starting at 50 mm. However, a strikingly lower foam formation is observed from a height of 60–70 mm. Especially for the frequencies 101 and 168 kHz, a later insonification was more effective for foam decay. Meanwhile, more foam developed throughout at the frequencies 42 and 85 kHz. This is most likely because some bubbles already reached the surface and formed foam before insonication started.

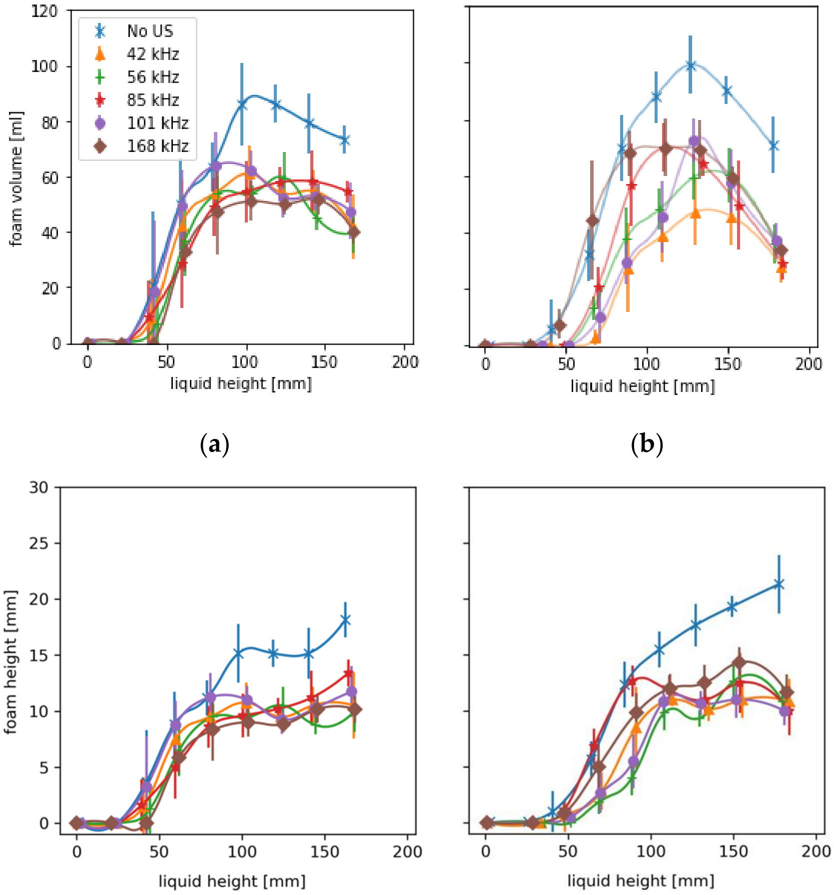

(**a**) (**b**)

(**c**) (**d**)

Figure 5. Effect of frequency depended ultrasound insonication with 2 s delay on the evolution of foam volume (**a**,**b**) and foam height (**c**,**d**) for apple juice (**a**,**c**) and currant nectar (**b**,**d**), each at 70 °C, n = 6.

3.2. Spatial and Temporal Effects

In addition to the respective heights in Figures 3 and 5, the captured images showed qualitative information on bubble rise and foam structure. The spatial change in bubble rise was already obvious at the beginning of filling at a liquid height of 30 mm, in which characteristic bubble-free areas are formed directly in front of the transducer and on the opposite side (Figure 6). Here, ultrasound caused pressure nodes and antinodes, which direct the bubbles through corridors to the surface. At the same time, the bubbles experience Bjerknes forces that first hold the bubbles in pressure antinodes and then cause two oscillating bubbles to coalesce [30,31]. This increases the ascent time directly due to the ultrasonic influence and indirectly due to the larger bubble diameter. As a result, the supply of new bubbles to the foam is interrupted, and the ratio of formation effects to decay effects decreases. This effect was evident again at a filling height of about 70 mm in the juices, where the transducer was lower than the liquid level and foam formation decreased (see Figures 3 and 5).

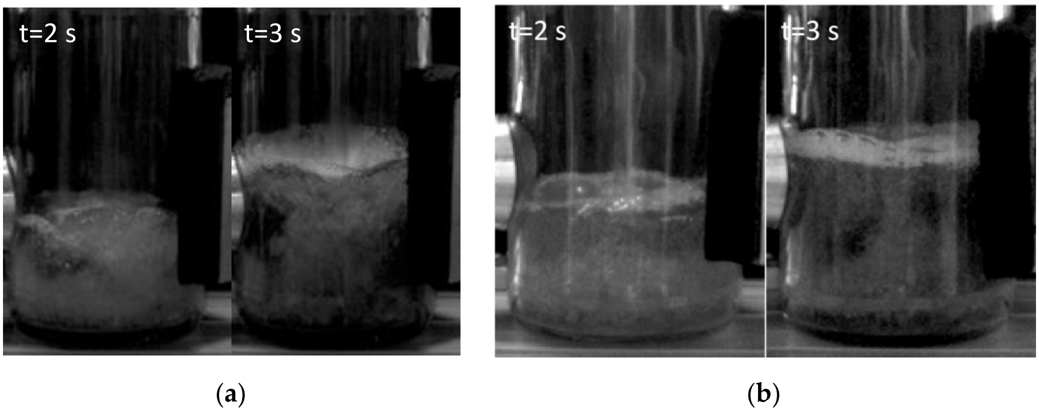

Figure 6. Bubble-free regions during filling time events t = 2 s and t = 3 s for apple juice at 45 kHz, 15 W (**a**) and unchanged bubble distribution without ultrasound (**b**).

The more effective the foam reduction by the ultrasound was, the drier and coarser the foams were by the end of filling. This was particularly evident in black currant nectar and apple juice, where defoaming was most effective (Figure 7). In return, the foams were denser when the ultrasonic effect was absent. Especially in apple juice, the coalescence of the bubbles happened in the end of the filling (Figure 7g–l). This also suggests the explanation that the larger rising bubbles coarsen the foam, thus minimizing its half-life. As a result, drier foams with lower foam heights are present towards the end of the filling process. These observations and the changed bubble rise in Figure 6 show that ultrasound already has an influence on the resulting foam during bubble ascent. However, low frequencies between 20 and 40 kHz bear the risk that, below a certain sound power, the pressure areas are not sufficiently developed in the liquid, whereby shear forces also caused by the sound waves are dominant. In this case, bubbles are dispersed, resulting in undesirable fine foams, as in the case of sonication of currant nectar at 42 kHz [31].

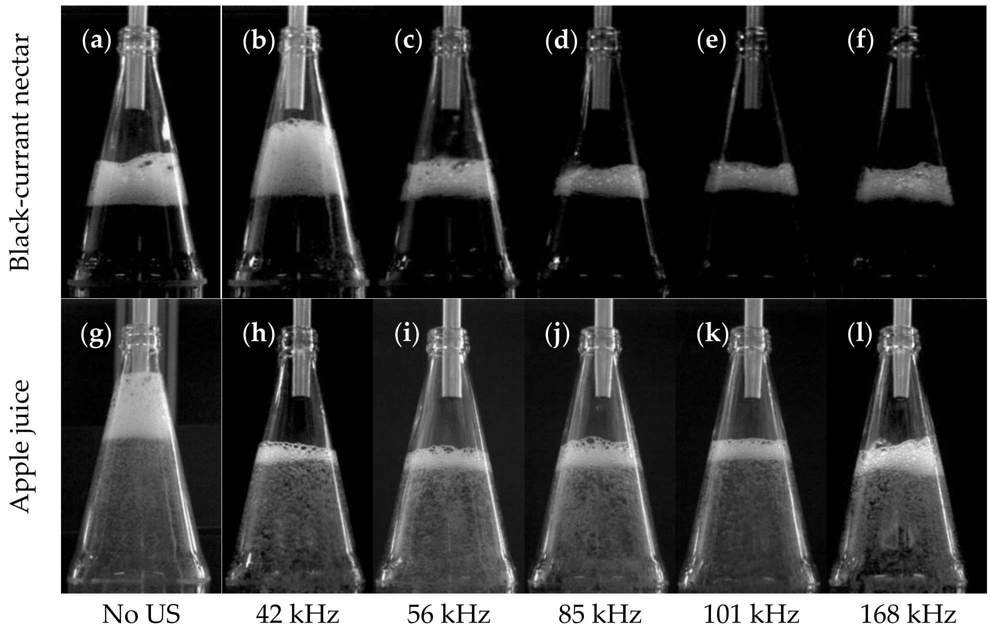

Figure 7. Insonification causes coarser, reduced foams of black currant nectar (**a**–**f**) and apple juice (**g**–**l**) and larger ascending bubbles in apple juice at the end of filling t = 10 s (**h**–**l**).

3.3. Reduced Half-Lives Due to Ultrasound

After filling, sonication continued for another 9 s at the respective frequency and power to enhance foam decay. At that point, no more gas bubbles ascended to the surface and no foam formation happened, resulting in pure foam decay.

The foam volume decayed exponentially during the observation time of 9 s according to the natural decay $V(\tau) = V_0 e^{-\lambda\tau}$, where V_0 is the respective foam volume directly after the end of filling, λ is the decay constant, and τ is the time in seconds after filling. The half-lives $\tau_{1/2} = \ln(2)/\lambda$ derived from this are shown normalized to half-lives of the reference foam of the respective juice in Figure 8. Here it became clear that sonication reduced the half-lives of the foam volume to between 63% (101 kHz) and 45% (85 kHz) in apple juice. The foams decayed completely except for a few individual foam bubbles. In the case of currant nectar on the other hand, the half-lives reduced to between 80% (101 kHz) and 57% (85 kHz), as the foam dried out quickly but larger bubbles remained. Nevertheless, the two juices showed similar frequency-dependent decay effects between 56 and 168 kHz.

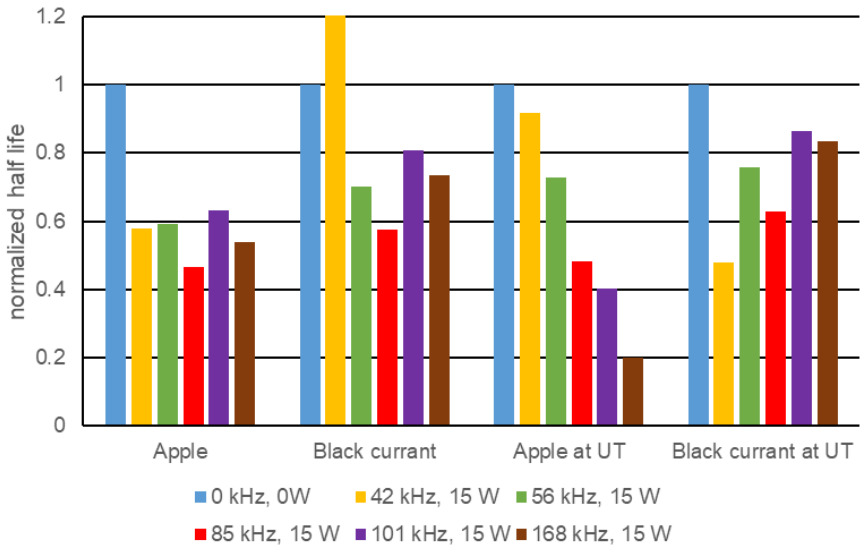

Figure 8. Normalized half-lives of the foams for all juices and frequencies related to reference half-lives (Apple: 5.5 s, black currant: 5.66 s, apple at UT: 8.77 s, black currant at UT: 4.5 s), n = 6.

4. Discussion

4.1. Impact of Liquid-Guided Ultrasound

In the experiments, the sonication occurred from the side through the bottle wall, whereby the waves propagated mostly below the foam due to the rising liquid height. It was reasoned that attaching the ultrasonic transducer to the bottle wall would overcome the severe acoustic impedance differences and high energy requirements of arrangements that included an air gap between the transducer and foam. In this respect, the required power of 15 W was far less than the 200 W of the airborne ultrasonic systems used to date [14–16]. This type of sonication differs from the common method, not only from the actuator design and power, but also from the defoaming behavior. The applied frequencies between 42 and 168 kHz might specifically induce resonant effects in the foam leading to higher drainage without atomization. These are well above the frequencies used by Winterburn [25], but within the range of McHardy [32].

The ratio of resonant bubble size to inserted frequency is simply assumed by the Rayleigh–Plesset frequency at first, assuming that the oscillation is linear and stable:

$$f_R = \frac{1}{2\pi r_R} \times \sqrt{\frac{3\gamma\left(p_0 + \frac{2\sigma}{r_R}\right) - \frac{2\sigma}{r_R}}{\rho_{Fluid}}} \quad (7)$$

The resonance radii are 76, 68, 57, 32, and 19 µm for f_R = [42, 56, 85 and 168 kHz] and surface tension σ of the corresponding juice, respectively. This range of resonant radii are to be considered in the first percentile when comparing bubble size distributions of juice foams after similar filling tests and bottle geometries [33]. Since foams become coarser towards the top, it can be assumed that such bubbles are more likely to be found on the bottom, inside Plateau-channels, or during early foam formation. Comparing the juices' surface tension at a particular frequency used in Equation (7), the shift of resonant radii is ± 1 µm, which means that the ultrasound/bubble interactions depend on the present bubble sizes rather than on the physical properties of juice. Therefore, the sonication is more effective when the ultrasound can reach the spot of resonant bubbles in the bottle. This effect is particularly evident above a filling height of 30 mm, where the actuator can first sonicate the bottom of the foam and the foam curves deviate from the reference measurements. This ultrasound method is most effective during the early phase of foam formation, when the bubbles were still spherical and freely moving. It can be assumed that, in this phase, the bubbles resonate by twice the usual resonant frequency due to their interacting acoustic influence [29]. The bubbles create surface waves during resonance enhance the flow around them. This causes a better drainage and coalescence already during foam development, resulting in coarser and more unstable foams by themselves.

In already existed foams, a subsequent sonication accelerates the decay (see Figure 8). Together, this results in a faster decay of the foam volume than in other experiments with subsequent sonication of already existing foams [32]. Because of the high reflections at and inside the foam, the sonication into the bottom of the foam may only penetrate into the first layers, where the liquid is removed more quickly. A downward sinking liquid gradient is created, which, in contrast to sonication from above, tends to remove the liquid from the plateau areas at the top [22].

The second influence is the standing wave formed within the liquid. It also showed a foam-avoiding effect in that smaller entrained bubbles passed through the pressure antinodes according to the applied frequency. In the presence of ultrasound in a gas-containing liquid, the bubbles can undergo either stable or transient cavitation. The bubbles undergoing stable oscillations grow to the resonance size or twice the resonance size by rectified diffusion or by coalescence due to the Bjerknes forces [34]. The bubble enlargements observed in Figure 7 can be explained by the fact that, at the applied sound pressures, the stably oscillating bubbles tend to grow by rectified diffusion and reach the resonance size [35,36]. This has a positive impact on foam prevention and should be achieved as early as possible in the process, for example by attaching the actuator to the bottle at a low level.

However, the applied acoustic pressures were not sufficient to subsequently destabilize the bubbles at resonance to the degree that they decayed into additional smaller bubbles and created transient cavitation (except for the run with 42 kHz and black currant nectar) [37–39]. Varying the test sequence for applied frequencies also showed no temporal effect on foam formation, which proved reversible effects of the sonication. Above the aforementioned sound pressures, defoaming effects slowly diminish or even reverse. It can be assumed that with increasing gas saturation of the liquid, this upper pressure limit decreases. Fruit juices have a very low saturation during production before bottling, which is why they have a higher upper pressure limit.

4.2. Industrial Feasibility

The method developed is for purely mechanical foam destruction using ultrasound to minimize product loss and filling times. The advantage over previous methods of foam prevention is that foam is already reduced in the bottle without the actuator being in direct contact with the product. In practice, rotary fillers and linear fillers inject the respective juice into bottles by moving the bottles to the filling spout via a height-adjustable positioning table. The ultrasonic actuator can be mounted at the positioning table and be in contact with the bottle via a waveguiding coupling material. Compared to an airborne ultrasonic defoamer with 200 W, 13 of such actuators can already control the foam in small fillers [15]. The actuator used generates low amplitudes, which meant that no abrasion could be detected on the bottle. The energy efficiency can still be optimized by switching to PET bottles with better transmission properties into the liquid or by improving the ultrasonic system. In the experimental setup presented, a parasitic series resistor was connected between the amplifier and the transducer. This compensated for the deviating electrical impedance mismatch of both components via thermal dissipation. An improved electrical circuit can lower that dissipation and improve the electrical efficiency of the ultrasonic system.

5. Conclusions

The results show the influence of sonication with ultrasound via the bottle wall on foam development during hot beverage filling at 70 °C. This type of sonication method differs from previous airborne ultrasonic systems due to higher frequencies and modest pressure amplitudes. The resonance effects in the bottom of the foam enhance the drainage and the decay, respectively. By avoiding transient cavitations, the juice is not degraded thermally or mechanically. The comparatively high frequencies between 42–168 kHz have an enhanced effect on wet, dense foams containing a large proportion of small resonant bubbles. A low power of 15 W was sufficient to change the rise of the entrained bubbles and minimize foam development right at the beginning. Compared to industrial airborne ultrasonic defoamers, the proposed method reduces foaming already during filling with 7.7% of the electrical power. Power dependence between 10–20 W and the harmonic relationship of the three most effective frequencies suggests a much stronger role of the natural frequencies of the liquid films or bubbles. The defoaming effects occurred mainly once the liquid level was above the ultrasonic actuator. The advantage of sonication over the liquid is that it more easily dries out, coarsens, and destabilizes wet foams. During filling, foams can be kept low and dry enough in a relatively short time window of a few seconds that little or no liquid can escape from the bottle and contaminate the plant.

The bottling experiments showed total foam reductions of more than 50% and shorter half-lives of the remaining foam of up to 55% in apple juice and currant nectar. The lowest effects of foam destruction occurred in orange juice, mainly due to the preventive effect pulp particles have on drainage. The experiments have been carried out on a commercial bottle geometry, proving its easy adaptability to industrial processes. However, further experiments on the influence of ultrasound on juices with higher viscosity, e.g., at lower temperature, or on other geometries should follow.

Author Contributions: J.T.; data curation, visualization, writing—original draft preparation, and investigation, B.G.; review and editing, supervision, and project administration; A.D.; conceptualization and writing—reviewing and editing. All authors have read and agreed to the published version of the manuscript.

Funding: This IGF Project of the FEI is funded via AiF (19711 N) within the program for promoting the Industrial Collective Research (IGF) of the German Ministry of Economic Affairs and Energy (BMWi), based on a resolution of the German Parliament.

Institutional Review Board Statement: Not applicable.

Informed Consent Statement: Not applicable.

Data Availability Statement: The data presented in this study are available on request from the corresponding author.

Acknowledgments: The authors thank Tobias Beck, Johannes Wiezcorek, and Stefanie Feilner for their support in the experimental measurements.

Conflicts of Interest: The authors declare no conflict of interest. The funders had no role in the design of the study; in the collection, analyses, or interpretation of data; in the writing of the manuscript; or in the decision to publish the results.

References

1. Voigt, T. *Neue Methoden für den Einsatz der Informationstechnologie bei Getränkeabfüllanlagen*; TU Munich: Munich, Germany, 2004.
2. Durand, M.; Langevin, D. Physicochemical approach to the theory of foam drainage. *Eur. Phys. J. E* **2002**, *7*, 35–44. [CrossRef]
3. Saint-Jalmes, A. Physical chemistry in foam drainage and coarsening. *Soft Matter* **2006**, *2*, 836–849. [CrossRef]
4. Koehler, S.A.; Stone, H.A.; Brenner, M.P.; Eggers, J. Dynamics of foam drainage. *Phys. Rev. E* **1998**, *58*, 2097. [CrossRef]
5. Cantat, I.; Cohen-Addad, S.; Elias, F.; Graner, F.; Höhler, R.; Pitois, O.; Rouyer, F.; Saint-Jalmes, A. *Foams: Structure and Dynamics*; OUP Oxford: Oxford, UK, 2013.
6. Boos, J.; Drenckhan, W.; Stubenrauch, C. On how surfactant depletion during foam generation influences foam properties. *Langmuir* **2012**, *28*, 9303–9310. [CrossRef]
7. Arteaga, G.; Nakai, S. Predicting protein functionality with artificial neural networks: Foaming and emulsifying properties. *J. Food Sci.* **1993**, *58*, 1152–1156. [CrossRef]
8. López-Barajas, M.; López-Tamames, E.; Buxaderas, S.; Suberbiola, G.; De la Torre-Boronat, M.C. Influence of wine polysaccharides of different molecular mass on wine foaming. *Am. J. Enol. Vitic.* **2001**, *52*, 146–150.
9. Dickinson, E. Food emulsions and foams: Stabilization by particles. *Curr. Opin. Colloid Interface Sci.* **2010**, *15*, 40–49. [CrossRef]
10. Murray, B.S.; Durga, K.; Yusoff, A.; Stoyanov, S.D. Stabilization of foams and emulsions by mixtures of surface active food-grade particles and proteins. *Food Hydrocoll.* **2011**, *25*, 627–638. [CrossRef]
11. Pahl, M.H.; Franke, D. Schaum und Schaumzerstörung–ein Überblick. *Chem. Ing. Tech.* **1995**, *67*, 300–312. [CrossRef]
12. Pugh, R. Foaming, foam films, antifoaming and defoaming. *Adv. Colloid Interface Sci.* **1996**, *64*, 67–142. [CrossRef]
13. Büttiker, A.; Keller, H.; Bates, D. Sonotrode and Device for Reducing and Eliminating Foaming of Liquid Products. U.S. Patent No 8,758,492, 24 June 2014.
14. Gallego-Juárez, J.A.; Rodriguez, G.; Acosta, V.; Riera, E. Power ultrasonic transducers with extensive radiators for industrial processing. *Ultrason. Sonochemistry* **2010**, *17*, 953–964. [CrossRef] [PubMed]
15. Riera, E.; Gallego-Juárez, J.A.; Mason, T.J. Airborne ultrasound for the precipitation of smokes and powders and the destruction of foams. *Ultrason. Sonochemistry* **2006**, *13*, 107–116. [CrossRef]
16. Sandor, N.; Stein, H.N. Foam Destruction by Ultrasonic Vibrations. *J. Colloid Interface Sci.* **1993**, *161*, 265–267. [CrossRef]
17. Bhakta, A.; Ruckenstein, E. Decay of standing foams: Drainage, coalescence and collapse. *Adv. Colloid Interface Sci.* **1997**, *70*, 1–124. [CrossRef]
18. Ross, S.; McBain, J. Inhibition of foaming in solvents containing known foamers. *Ind. Eng. Chem.* **1944**, *36*, 570–573. [CrossRef]
19. Sun, S.C. Destruction of flotation froth with intense high frequency sound. *Min. Eng.* **1951**, *3*, 865–867.
20. Dorsey, A.E. Control of foam during fermentation by the application of ultrasonic energy. *J. Biochem. Microbiol. Technol. Eng.* **1959**, *1*, 289–295. [CrossRef]
21. Boucher, R.; Weiner, A. Foam control by acoustic and aerodynamic means. *Br. Chem. Eng.* **1963**, *8*, 808–812.
22. Dedhia, A.C.; Ambulgekar, P.V.; Pandit, A.B. Static foam destruction: Role of ultrasound. *Ultrason. Sonochemistry* **2004**, *11*, 67–75. [CrossRef]
23. Morey, M.; Deshpande, N.; Barigou, M. Foam destabilization by mechanical and ultrasonic vibrations. *J. Colloid Interface Sci.* **1999**, *219*, 90–98. [CrossRef] [PubMed]
24. Chendke, P.; Fogler, H.S. Second-order sonochemical phenomena—Extensions of previous work and applications in industrial processing. *Chem. Eng. J.* **1974**, *8*, 165–178. [CrossRef]
25. Winterburn, J.B.; Martin, P.J. Mechanisms of ultrasound foam interactions. *Asia-Pac. J. Chem. Eng.* **2009**, *4*, 184–190. [CrossRef]
26. Leroy, V.; Fan, Y.; Strybulevych, A.L.; Bellido, G.G.; Page, J.H.; Scanlon, M.G. Investigating the bubble size distribution in dough using ultrasound. *Bubbles Food* **2008**, *2*, 51–60.
27. Gómez, M.; Oliete, B.; García-Álvarez, J.; Ronda, F.; Salazar, J. Characterization of cake batters by ultrasound measurements. *J. Food Eng.* **2008**, *89*, 408–413. [CrossRef]
28. McClements, D.J.; Gunasekaran, S. Ultrasonic characterization of foods and drinks: Principles, methods, and applications. *Crit. Rev. Food Sci. Nutr.* **1997**, *37*, 1–46. [CrossRef]
29. Leroy, V.; Strybulevych, A.; Scanlon, M.G.; Page, J.H. Transmission of ultrasound through a single layer of bubbles. *Eur. Phys. J. E* **2009**, *29*, 123–130. [CrossRef]
30. Leighton, T. *The Acoustic Bubble*; Academic Press: Cambridge, MA, USA, 2012.
31. Vo, H.S.; Kentish, S.; Ashokkumar, M. The enhancement of foam generated by low power ultrasound and its application to foam fractionation. *Colloids Surf. A Physicochem. Eng. Asp.* **2011**, *380*, 35–40. [CrossRef]
32. McHardy, C.; Thünnesen, J.; Horneber, T.; Kostova, J.; Hussein, M.A.; Delgado, A.; Rauh, C. Active control of foams by physically based destruction mechanisms. *PAMM* **2018**, *18*, e201800351. [CrossRef]
33. Panckow, R.P.; McHardy, C.; Rudolph, A.; Muthig, M.; Kostova, J.; Wegener, M.; Rauh, C. Characterization of fast-growing foams in bottling processes by endoscopic imaging and convolutional neural networks. *J. Food Eng.* **2021**, *289*, 110151. [CrossRef]
34. Vaidya, H.A.; Ertunç, Ö.; Lichtenegger, T.; Hachmann, J.; Delgado, A.; Skupin, A. High-speed visualization of acoustically excited cavitation bubbles in a cluster near a rigid boundary. *J. Vis.* **2017**, *20*, 359–368. [CrossRef]
35. Eller, A.; Flynn, H. Generation of subharmonics of order one-half by bubbles in a sound field. *J. Acoust. Soc. Am.* **1969**, *46*, 722–727. [CrossRef]
36. Crum, L. Acoustic cavitation series: Part five rectified diffusion. *Ultrasonics* **1984**, *22*, 215–223. [CrossRef]

37. Neppiras, E.A. Acoustic cavitation. *Phys. Rep.* **1980**, *61*, 159–251. [CrossRef]
38. Neppiras, E. Subharmonic and other low-frequency emission from bubbles in sound-irradiated liquids. *J. Acoust. Soc. Am.* **1969**, *46*, 587–601. [CrossRef]
39. Sato, M.; Shibuya, N.; Okada, N.; Tou, T.; Fujii, T. Oscillation mode conversion and energy confinement of acoustically agitated bubbles. *Phys. Rev. E* **2002**, *65*, 046302. [CrossRef] [PubMed]